Arctic Science

OPEN ACCESS | Article

The spatial and temporal influence of infrastructure and road dust on seasonal snowmelt, vegetation productivity, and early season surface water cover in the Prudhoe Bay Oilfield

Helena Bergstedt[a,c], **Benjamin M. Jones**[a], **Donald Walker**[b], **Jana Peirce**[b], **Annett Bartsch**[c], **Georg Pointner**[c], **Mikhail Kanevskiy**[a], **Martha Raynolds**[b], **and Marcel Buchhorn**[d]

[a]Institute of Northern Engineering, University of Alaska Fairbanks, Fairbanks, AK 99775, USA; [b]Institute of Arctic Biology, and Department of Biology and Wildlife, University of Alaska Fairbanks, Fairbanks, AK 99775, USA; [c]b.geos, 2100 Korneuburg, Austria; [d]Remote Sensing Unit, Flemish Institute for Technological Research (VITO), B-2400 Mol, Belgium

Corresponding author: **Helena Bergstedt** (email: helena.bergstedt@bgeos.com)

Abstract

Increased industrial development in the Arctic has led to a rapid expansion of infrastructure in the region. Localized impacts of infrastructure on snow distribution, road dust, and snowmelt timing and duration feeds back into the coupled Arctic system causing a series of cascading effects that remain poorly understood. We quantify spatial and temporal patterns of snow-off dates in the Prudhoe Bay Oilfield, Alaska, using Sentinel-2 data. We derive the Normalized Difference Snow Index to quantify snow persistence in 2019–2020. The Normalized Difference Vegetation Index and Normalized Difference Water Index were used to show linkages of vegetation and surface hydrology, in relationship to patterns of snowmelt. Newly available infrastructure data were used to analyze snowmelt patterns in relation infrastructure. Results show a relationship between snowmelt and distance to infrastructure varying by use and traffic load, and orientation relative to the prevailing wind direction (up to 1 month difference in snow-free dates). Post-snowmelt surface water area showed a strong negative correlation (up to −0.927) with distance to infrastructure. Results from field observations indicate an impact of infrastructure on winter near-surface ground temperature and snow depth. This study highlights the impact of infrastructure on a large area beyond the direct human footprint and the interconnectedness between snow-off timing, vegetation, surface hydrology, and near-surface ground temperatures.

Key words: Infrastructure, remote sensing, snow, permafrost, hydrology

1 Introduction

Arctic regions are experiencing rapid change due to cumulative effects caused by climate change and the expansion of infrastructure driven primarily by industrial development related to resource extraction (NRC 2003; AMAP 2007; Walker et al. 2022). Oil and gas exploration and development, in particular, has led to the spread of infrastructure in many areas of the circumpolar Arctic over the last five decades (Kumpula et al. 2012; Raynolds et al. 2014, 2020; Walker et al. 2022). Areas like the Prudhoe Bay Oilfield (PBO) in Alaska (Fig. 1A) are host to many types of infrastructure, ranging from paved and gravel roads, airports, stores, and other service facilities, to pipelines, processing plants, drill rigs, gravel pits and pads, and associated features of oil and gas production (Raynolds et al. 2014). Studies documenting increased infrastructure development in the area of Prudhoe Bay have shown that it impacts the surrounding natural environment in multiple ways, including changes to hydrology, soils, vegetation, permafrost, snowmelt, and ground temperatures (Benson et al. 1975, Walker et al. 1980;, 2022; Walker 1985; Walker and Everett 1987; Raynolds et al. 2014; Kanevskiy et al. 2022).

Infrastructure actively influences the distribution and redistribution of snow by creating barriers that act like snow fences, leading to modified snow depths and snowmelt patterns (Fortier et al. 2011). Previous studies have shown that snow along roads and on road embankments can disappear earlier compared to snow in the surrounding area, leading to earlier soil thaw and vegetation green-up near roads (Benson et al. 1975; Walker and Everett 1987; Walker et al. 2022; Chen et al. 2020).

In winter, roadside snow drifts develop along the margins of the elevated roads. Heavily traveled roads, such as the Spine Road and the Dalton Highway, also collect large quantities of dust during the winter and spring. These large amounts of dust decrease the albedo of snow which induces

long-term records for the Northern Hemisphere covering a period starting in 1979 (Takala et al. 2011).

Studies based on multispectral data as well as those based on microwave remote sensing systems lack either the spatial or temporal resolution to adequately assess the impact of separate infrastructure units on the surrounding environment on an annual basis. Data products like the MODIS snow coverage maps provide daily global measurements in 500 m spatial resolution. While the daily temporal resolution provides many advantages for timely analysis of snow cover, the impact of local infrastructure on the direct environment cannot be fully captured with this coarse spatial data. Other products such as the GlobSnow (Takala et al. 2011) are available in 1 km to 250 m resolution versions. Snow mapping efforts based on Landsat imagery have the advantage of higher spatial resolution (30 m). Macander et al. (2015) calculated the typical snow-free date for Northwest Alaska based on Landsat imagery from 1985 to 2011 (Fig. 1*b*). Snowmelt patterns in Arctic landscapes have also been studied on a local level using time-lapse cameras (e.g., Kępski et al. 2017) and in situ sensor observations. Sentinel-2 and the Normalized Difference Snow Index (NDSI) have been used successfully to map snow cover in alpine areas (Gascoin et al. 2020); however, studies using Sentinel-2 to map snow in tundra environments are currently lacking, to the best of our knowledge. Sentinel-2 allows for mapping snow cover at high spatial resolution (20 m) and offers the possibility of acquisition with a 5 day interval over the study area (Drusch et al. 2012; Gascon et al. 2017).

The ability to accurately map and monitor the expansion of infrastructure in the Arctic is important for assessing and mitigating risks to and from infrastructure in a climate that is warming three times faster than other places on earth (Walker and Peirce 2015). Approaches for mapping infrastructure using remote sensing have been widely studied on a global and local scale (Bartsch et al. 2020). Infrastructure and its impacts on Arctic environments can be assessed by remotely sensed methodologies. Several data sets based on remote sensing data with regional to global coverage exist (e.g., Wang et al. 2017; Esch et al. 2018), but often lack either comprehensive documentation of different types of infrastructure or suitable coverage of Arctic settlements and infrastructure hubs (Bartsch et al. 2020). Recent advancements have allowed for high spatial resolution mapping (10 m) of both linear infrastructure (e.g., roads) and built-up areas on a circumpolar scale based on Synthetic Aperture Radar and multispectral data acquired by the Sentinel-1 and Sentinel-2 constellations (Sentinel-1/2-derived arctic coastal human impact data set (SACHI); Bartsch et al. 2020).

In this study, we describe and quantify spatial and temporal patterns of snowmelt timing in relation to infrastructure in the Prudhoe Bay area. We demonstrate the potential of resources like the Sentinel-2 constellation to quantify and monitor snowmelt patterns in Arctic industrial regions as well as the resulting cumulative effects of infrastructure development on hydrology and vegetation. This study addresses multiple themes, focussing on connectivity of different landscape elements, connected to the Terrestrial Multidisciplinary distributed Observatories for the Study of Arctic Connections initiative (Vincent et al. 2019), making it highly relevant for the future study of Arctic natural and social systems.

2 Methods

2.1 Study area

The study area for this analysis spans across Deadhorse and parts of the PBO on the North Slope of Alaska (see Fig. 1*a*). The area is located on the Beaufort Sea coast, delineated by the Sagavanirktok River to the east and the Kuparuk River to the west. The area has experienced extensive infrastructure development since the 1960s (Raynolds et al. 2014). Infrastructure in the area includes roads and bridges, buildings, airports, and oil and gas infrastructure. The area including PBO is generally flat, and infrastructure creates significant local relief.

2.2 Data

2.2.1 Remote sensing

The remote sensing analysis in the study was based on multispectral data from the Sentinel-2 constellation from 2019 to 2020 (Drusch et al. 2012). Sentinel-2 acquisitions are offered at different levels of processing with Level-1 C, providing radiometrically and geometrically corrected Top of Atmosphere (TOA) reflectance values. Spatial resolution differs between the bands ranging from 10 to 60 m. The spatial resolution depends on the band, with four bands having a spatial resolution of 10 m, six bands of 20 m and three bands of 60 m. Sentinel-2 Level-2 A data were not available for our study area prior to December 2018; therefore, Level-1 C data were utilized for the entire study period. For an overview of the general methodologies, see Fig. 2.

2.2.2 Infrastructure

The comprehensive SACHI (Bartsch et al. 2021*a*; *b*), including roads, built-up areas, and pipelines, was used in this study to relate the presence of infrastructure and snowmelt patterns across the Prudhoe Bay area (Fig. 3). The infrastructure data set was created using both Sentinel-1 and Sentinel-2 data, being produced at a 10 m spatial resolution. For further description of the infrastructure layer development, see Bartsch et al. 2020.

To examine the influence of different types of infrastructure on snowmelt patterns, the data set was manually edited, and roads and pipelines were split at intersections. Larger infrastructure areas were split from connecting roads (where this was not already the case in the original data layer) to allow for separate analysis of roads, pipelines, and other infrastructure types.

2.2.3 Road construction and maintenance: ice paving, snow removal, and winter dust abatement

Roads in the PBO are classified as primary, access, flowline and other. In an interview with Hilcorp's field opera-

Fig. 2. Workflow diagram, including input data, processing steps and main output variables. NDSI, Normalized Difference Snow Index; NDVI, Normalized Difference Vegetation Index; NDWI, Normalized Difference Water Index; SACHI, Sentinel-1/2-derived arctic coastal human impact data set.

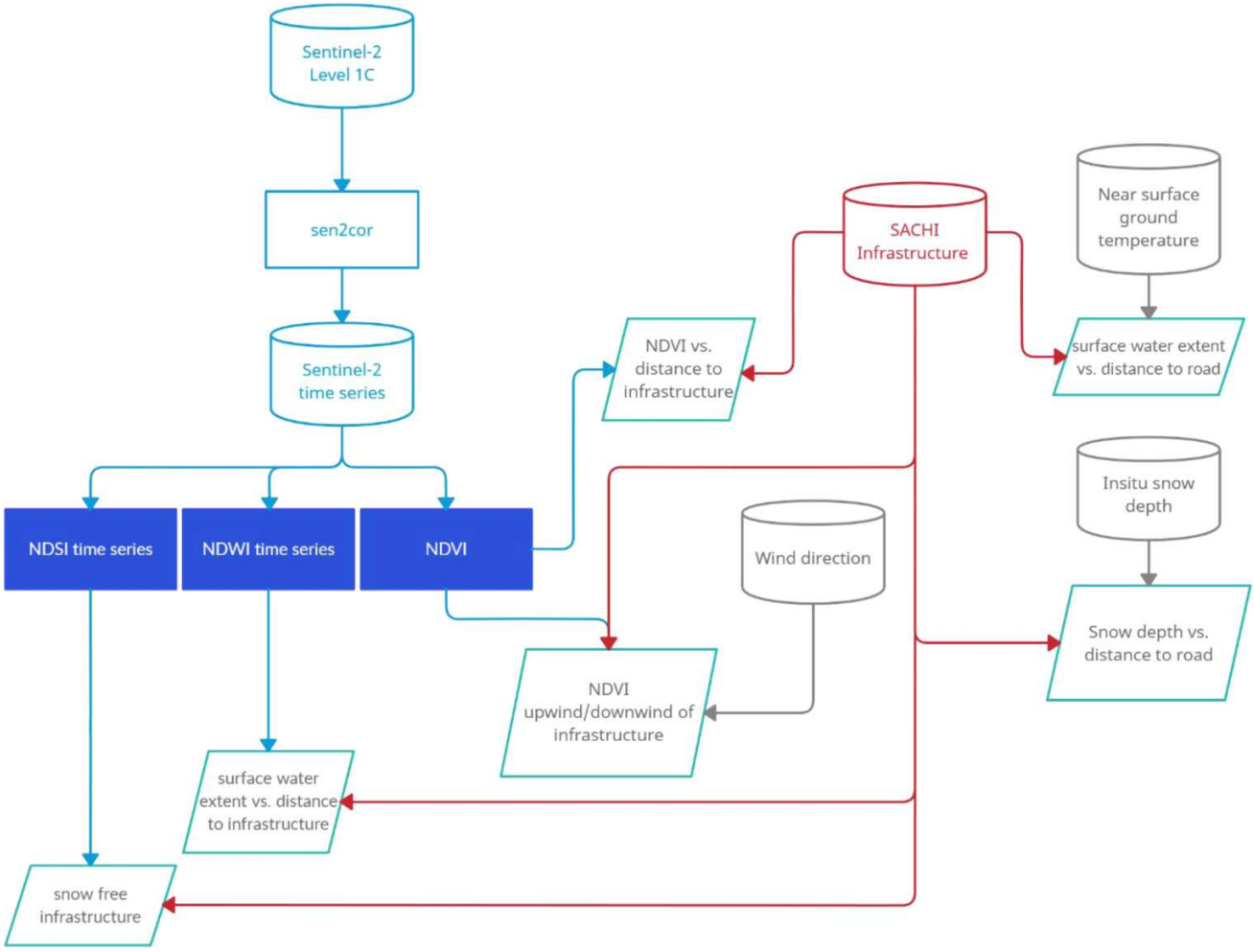

tions supervisor for oilfield roads and pads, information was obtained on road construction and maintenance practices that impact snow-off dates, including road elevation and snow removal. Dust abatement practices were also discussed. This information was then further used to choose selected road segments experiencing high traffic volume, which were expected to have relatively high dust occurrence compared to less used road segments.

2.2.4 In situ snow and temperature measurements

Near surface ground temperature was measured from July 2015 to July 2016 on four different transects (T1–T4) in the Deadhorse area (Fig. 3). Transects were perpendicular to the road and reached up to 200 m. Temperatures were recorded using iButton temperature sensors at 4 hour intervals, at distances 0, 5, 10, 25, 50, 100 and 200 m from the road. Daily averages for near surface ground temperatures were calculated from all available measurements.

Snow depth measurements were collected in March 2016 along these four transects, every meter along the first 100 m of T1 and T2, then every 5 m from 105 to 200 m. On T3 and T4, which are 100 m long, snow depth was measured every meter.

2.2.5 Wind

Wind speed and wind direction information was retrieved for the Deadhorse weather station (ID: USW00027406, located at the airport, see Fig. 3) from the National Oceanic and Atmospheric Administration climate database. The Deadhorse weather station provides daily mean values for wind speed and dominant wind direction.

2.3 Data processing

As Sentinel-2 data were available for TOA reflectance only, atmospheric correction and cloud masking were required prior to further analysis. Available images were inspected visually for clouds and cloud shadows and excluded if necessary. Level-1 C data were atmospherically corrected and transformed to Level-2 A data using the sen2cor processing module integrated in the Sentinel Application Platform

Fig. 3. Infrastructure (Bartsch et al. 2021*a*) based on Sentinel-2 imagery in the Prudhoe Bay area, including place names mentioned in the text. Established transects 1, 2, 3, and 4 (in panels B and C; referred to in the text as T1–T4) where surface temperature and snow depth were recorded; transects 1 and 2 are 200 m long, transects 3 and 4 are 100 m long (sources for background imagery: Esri, DigitalGlobe, GeoEye, i-cubed, USDA FSA, USGS, AEX, Getmapping, Aerogrid, IGN, IGP, swisstopo, and the GIS User Community) (sources for grey basemap: Esri, DeLorme, HERE, MapmyIndia (WGS84/Alaska Polar Stereographic))

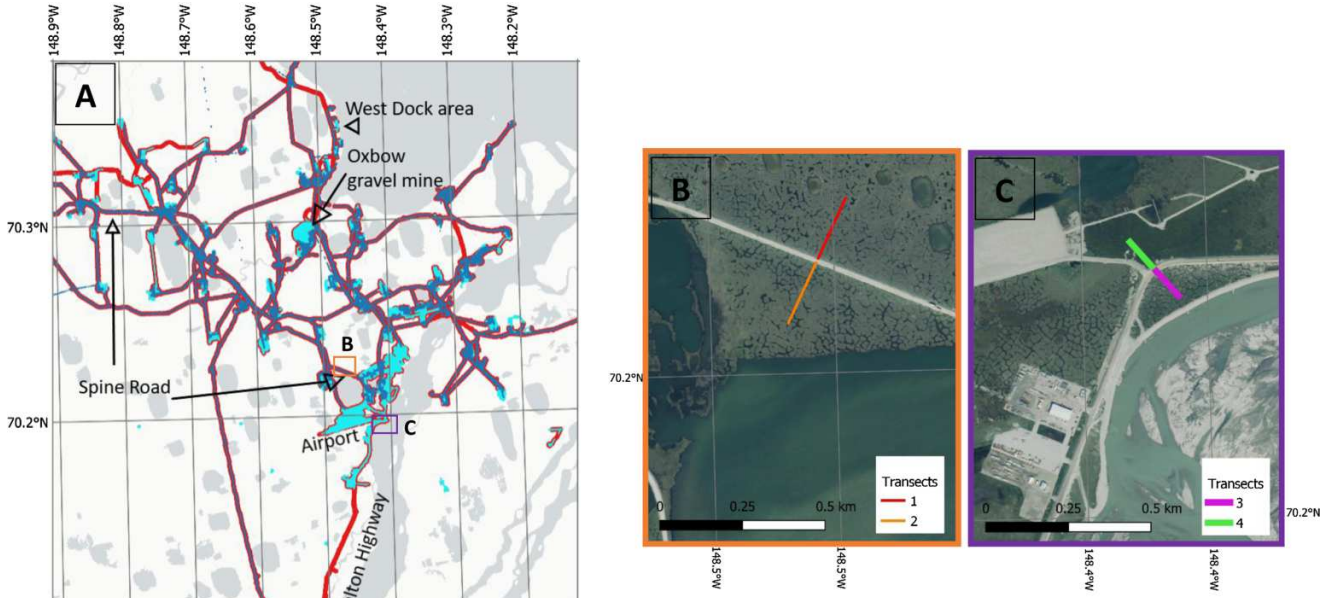

(https://step.esa.int/main/download/snap-download/) software package. Sen2cor also created a cloud mask, which was used for masking partially cloudy imagery to maximize the number of available acquisitions per pixel.

2.4 Analysis

To quantify snow cover on a pixel basis, we used the NDSI derived from Sentinel-2 imagery from January to June for years 2019–2020. The NDSI has been used on many occasions to assess and map snow extent in arctic and alpine environments (Dozier 1989; Salomonson and Appel 2004; Chaponnière et al. 2005; Aalstad Westermann and Bertino 2020). The NDSI is calculated as a ratio, including the green (Band 3) and short wave infrared (Band 11) bands (20 m resolution).

$$NDSI = \frac{Band3 - Band11}{Band3 + Band11}$$

Pixels with NDSI values above a threshold of 0.4 were considered snow covered. The threshold value of 0.4 was chosen in accordance with existing literature (Macander et al. 2015) and visual interpretation of NDSI and Sentinel-2 imagery in the study area. To determine the snow-free dates per pixel for each year, time series of NDSI values were created. For each pixel, the snow-free date was defined as the first time when a pixel's NDSI value was below the threshold value of 0.4.

Median NDSI values in the two months prior to snowmelt onset (February–March) were used to determine which sections of infrastructure were snow covered or snow free during winter. The snow-free threshold of 0.4 was applied to the NDSI values which were extracted for the infrastructure data set. Sections of infrastructure were classified as snow free when median NDSI values were below 0.4, as partially snow-covered for infrastructure segments with NDSI values close to the threshold (0.4–0.45) and as snow-covered when median NDSI values were above 0.4.

To include surface water and hydrological aspects into our analysis, we derived the Normalized Difference Water Index (NDWI) from the Sentinel-2 imagery from June acquisitions. The NDWI has been used successfully in the past to map and quantify surface water (Du et al. 2016; Nitze and Grosse 2016). The NDWI is calculated as a ratio of the green (Band 3) and near infrared (NIR, Band 8) bands (10 m resolution).

$$NDWI = \frac{Band3 - Band8}{Band3 + Band8}$$

To achieve the best possible spatial coverage of NDWI values, a median composite was created from all available June imagery. The threshold for distinguishing water areas from surrounding landscapes was decided by visual interpretation of the imagery and set to an NDWI value of 0.05.

To include aspects of vegetation into our analysis, we derived the Normalized Difference Vegetation Index (NDVI)

from the Sentinel-2 imagery from May–September for the years 2016–2020. The NDVI is calculated as a ratio of the NIR (near infrared, Band 8) and red (Band 4) bands (10 m resolution).

$$NDVI = \frac{Band8 - Band4}{Band8 + Band4}$$

To compare the progression of NDVI over the growing season, areas upwind and downwind of roads were investigated separately. In addition, maximum NDVI and median NDVI for July–August acquisitions were compared to snow-free dates on a pixel basis for selected sites within the study area. These sites were selected to represent areas close to different types of infrastructure (e.g., roads, pipelines, gravel pads, and gravel pits).

3 Results

3.1 Snow-free dates 2019–2020

Spatial patterns of snow-free timing were visible for all 5 years of observation, derived from Sentinel-2 based NDSI indices. Snow-free dates for the Prudhoe Bay area for the years 2019 and 2020, are shown in Fig. 4. Snow-free dates varied for different areas within the study sites as well as between the different years included in this analysis. Zoomed in panels in Fig. 4 highlight the spatial variability of snow-free dates over the study area for 2019 and 2020. Overall snow-free dates in 2020 show less spatial variability than 2019; however, similarities are visible for both years. Later snowmelt along the Trans-Alaska Pipeline is distinct in both years (highlighted by gray ellipse in Fig. 4).

Relating snow-free dates on a pixel basis to the distance to the nearest infrastructure showed little difference in median values., Pixels within 5 km of roads or pipelines showed a larger spread of snow-free dates and outliers compared to pixels further from nearest infrastructure, and noticeable occurrences of earlier snow-free dates (Figs. 5 and 6). For 2019 the results show a larger number of later snow-free dates for pixel within 100 m to roads and pipelines (Figs. 5 and 6). For a selected road section with high traffic volume there are strong differences in snow-free dates with distance to the nearest road segment (Fig. 7). For both 2019 and 2020, pixels downwind of the road show fewer outliers and larger differences in snow-free dates between pixels near and further from the road compared to upwind pixels. In 2019 pixels downwind from the road segment show snow-free dates before day 130 (DOY) for pixels closest to the road, and snow-free dates greater after DOY 160 for pixels within 350-375 m distance of the road, a difference of approximately 1 month (Fig. 7).

3.2 Snow cover of infrastructure

Snow cover of infrastructure prior to snowmelt was determined from February to March NDSI values for the infrastructure data set for the Prudhoe Bay area (Fig. 8). Areas with heavy traffic, such as the airport runway, parts of gravel mines and of other oil and gas infrastructure were snow free prior to snowmelt. In addition, sections of the Spine Road (the main east–west road in the PBO), the road leading to the Oxbow gravel mine, the West Dock area, and parts of the Dalton Highway were snow free (for place names see Fig. 3). Pipelines, smaller roads and most gravel pads, and built-up areas were snow covered prior to snowmelt onset.

3.3 Temperature, snow depth, and wind data analysis

Near surface ground temperature data (Walker et al. 2022) for the four transects showed higher winter values (January through March) at 5 m distance from the road compared to data recorded at larger distances, and less variation during winter months at all sites and distances compared to summer months (Fig. 9). The difference between measurements at 5 m and those at larger distances was especially pronounced for transects with extensive flooding on the downwind side of the road and deeper snow (T2 and T4).

In situ snow depth for March 2016 for transects 1–4 showed decreasing snow depth with distance from road (Fig. 10). Snow depth near the road reached up to 100 cm. See Fig. 10 for individual transect measurements.

Predominant wind directions for the Deadhorse weather station were analysed for separate years and separate months from 2015 to 2020 (Fig. 11). The strongest winds occurred in April, May, and June (Fig. 11, left-hand side). Dominant wind directions were somewhat consistent over different years, with the prevailing winds coming from a North–East direction (Fig. 11, right-hand side). Comparing dominant wind directions for different months revealed similar patterns, however there was more variability between different months compared with different years.

In both 2019 and 2020, snow-free dates were later on the downwind side of infrastructure than on the upwind side, and were even later for distances over 300 m on the downwind side of the road (Fig. 7).

3.4 Normalized Difference Vegetation Index

Median 2016–2020 July NDVI in relation to the distance to roads and pipelines in the study area did not show strong differences in values between areas close and further away from infrastructure (Fig. 12), though sections closest to the road showed slightly higher values. Comparing downwind and upwind areas of roads in the study area showed lower NDVI values for downwind areas early in the growing season and higher NDVI values later in the growing season (Fig. 13). Maximum NDVI values for 2019 and 2020 showed weak correlations (0.16 for 2019 and 0.18 for 2020) with DOY of a pixel becoming snow free (Fig. 14).

3.5 Surface water area post snowmelt

June surface water area derived from NDWI values showed strong negative correlation with the distance to infrastructure (Fig. 15). Surface water area was correlated with the distance from the road with a correlation coefficient of −0.927 (−0.928 for pipelines and −0.886 for other areas, Fig. 15). While the correlation was strongest for roads, all three types of infrastructure show a strong relationship of water area and

Fig. 4. Snow-free dates (SFD) for 2019 (A) and 2020 (B) for the Prudhoe Bay area derived from Sentinel-2 NDSI values. Yellow (later date) NNW-SSE line (highlighted by gray ellipse) in center of image is caused by the Trans-Alaska Pipeline. Panels C–F show zoomed in versions for 2019 (C and E) and 2020 (D and F) for the areas highlighted by the grey rectangles. Panel 4B shows evidence of the importance of acquisition dates, with visible differences in detected snow-free dates between east and west caused by image availability (sources for grey basemap: Esri, DeLorme, HERE, and MapmyIndia) (WGS84/Alaska Polar Stereographic). NDSI, Normalized Difference Snow Index.

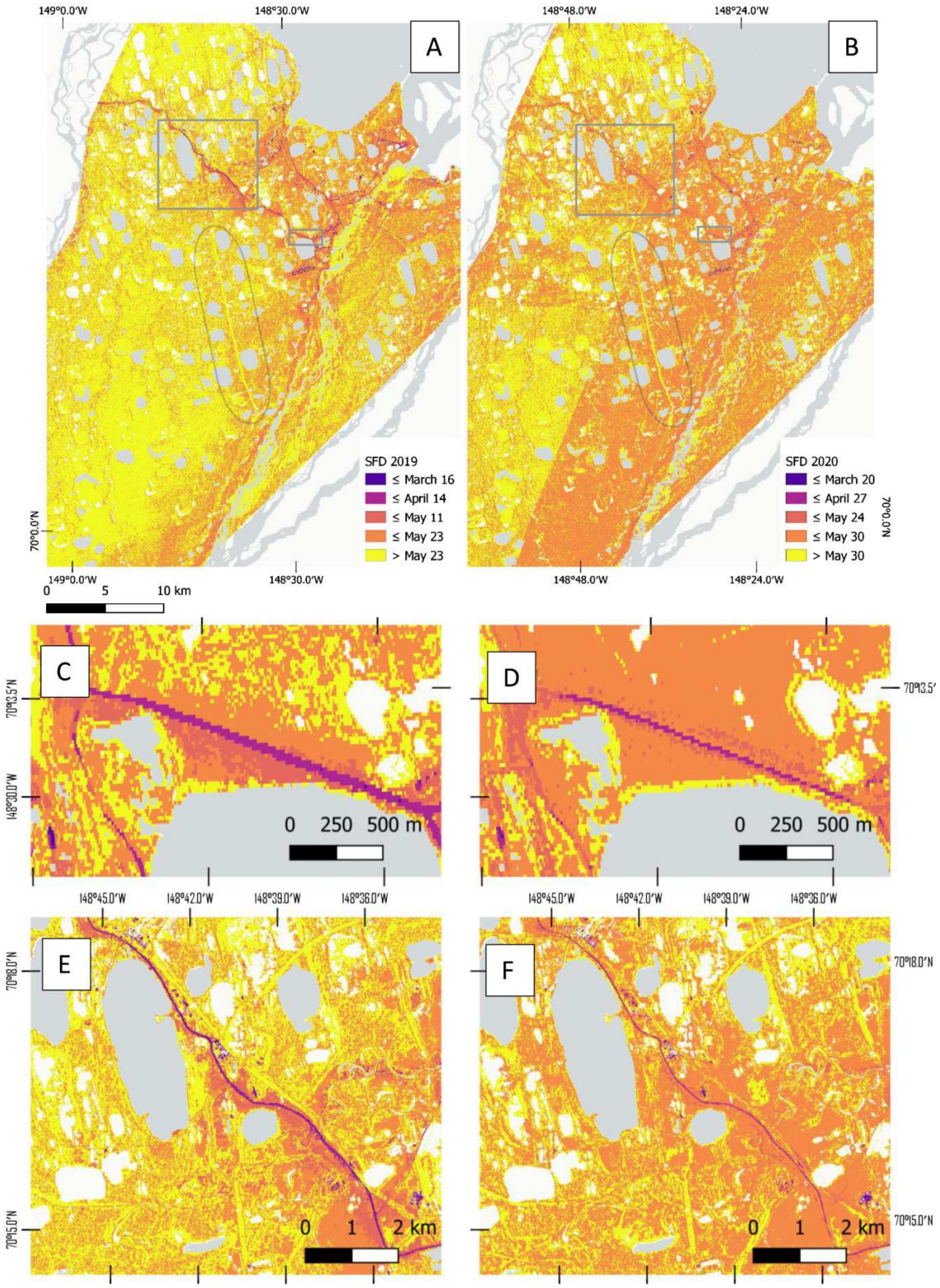

Fig. 5. First snow-free DOY for 2019 (A) and 2020 (B) per Sentinel-2 pixel in relationship with pixel distance to nearest road in the Prudhoe Bay area, Alaska (50 m bins). The values below the medians are earlier snow-free dates. DOY, day of year.

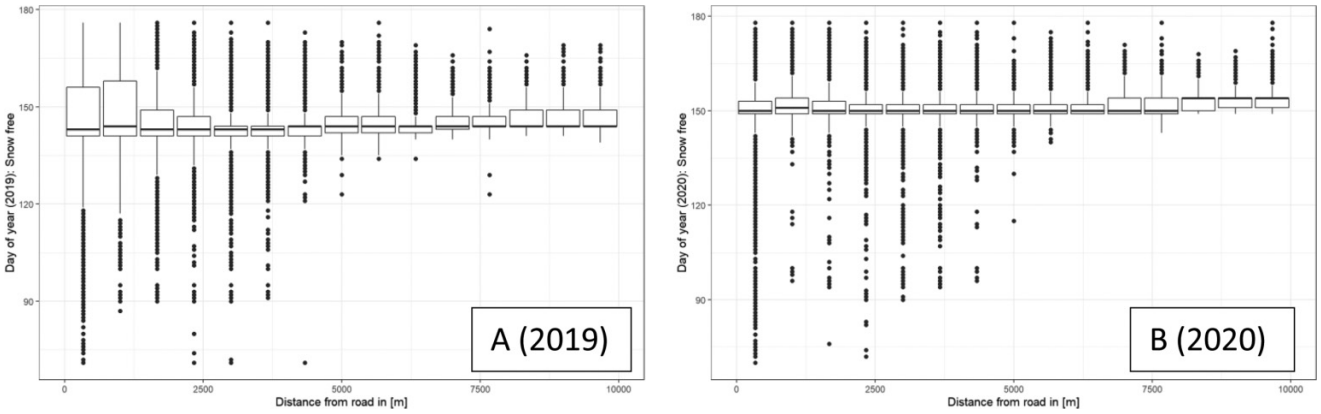

Fig. 6. First snow-free day of year for 2019 and 2020 per Sentinel-2 pixel in relationship with pixel distance to nearest pipeline in the Prudhoe Bay area, Alaska (50 m bins). The values below the medians are earlier snow-free dates.

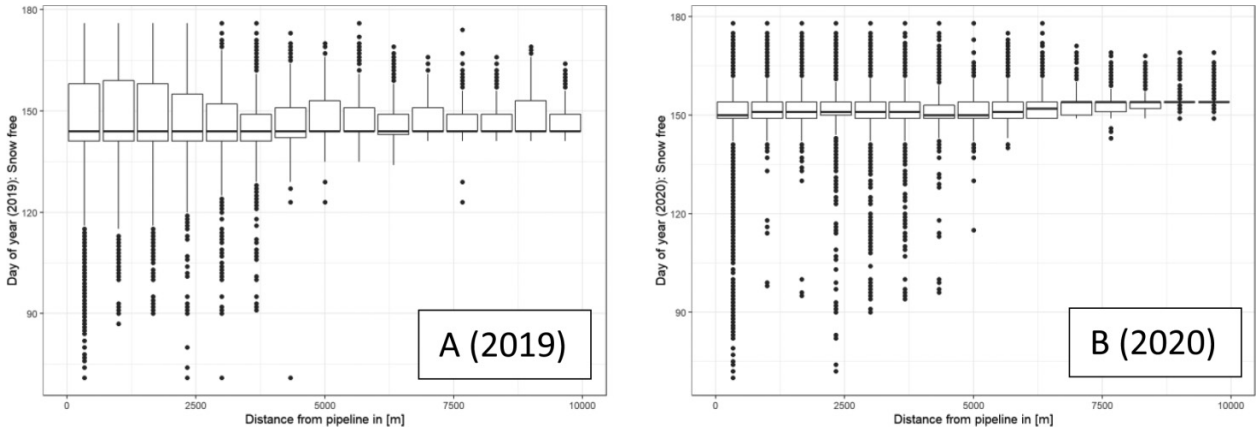

distances to infrastructure. For all roads, pipelines, and areas, the surface water area is higher closer to the road.

4 Discussion

Spatial patterns in snow cover and snow-free dates are visible in the results based on Sentinel-2 derived NDSI. Depending on data availability and cloud conditions, the Sentinel-2 constellation provides acquisitions over the Prudhoe Bay area 1–2 times per week. This is a relatively high temporal resolution compared to other multispectral satellite data sets with comparable spatial resolution (e.g., Landsat satellites). After the launch of Sentinel-2B in March 2017, the second satellite in the constellation, the temporal resolution improved significantly. Earlier years did not have enough temporal or spatial coverage of the study area during the relevant time frames to adequately derive snowmelt timing.

Even though the temporal resolution was theoretically adequate to detect snow-free patterns over the study area after 2017 areas might become snow free between cloud free satellite acquisitions, especially toward the end of snowmelt, when melting progresses quickly. Therefore, some fine scale spatial patterns may be missed (Fig. 4B). For our analysis, due to cloud cover and gaps between acquisitions, sufficient imagery during the snowmelt period was only available during 2019 and 2020. The spatial patterns in this study showed earlier snowmelt for locations adjacent to roads and revealed linear features associated with later snow-free dates. These delayed snowmelt features represent large snowdrifts associated with elevated pipelines and roads, with the Trans-Alaska Pipeline specifically standing out (Fig. 4). This can be confirmed through field observations shown in Fig. 16. Both photographs in Fig. 16 show clear delayed snowmelt along pipeline features with Fig. 16B depicting delayed snowmelt along the Trans-Alaska Pipeline.

Previous studies that mapped snow-free dates for the region showed similar patterns of earlier snowmelt in the Prudhoe Bay area compared to surrounding areas less impacted by infrastructure and oil development (Macander et al. 2015). In addition, the study by Macander et al. (2015) showed similar patterns of later snowmelt surrounding the Trans-Alaska Pipeline, supporting our findings (see Figs. 2 and 4).

Fig. 7. First snow-free DOY for 2019 and 2020 per Sentinel-2 pixel in relationship with pixel distance to nearest road segment (25 m bins), downwind (left) and upwind (right). A and B: entire study area; C and D: downwind and upwind of road segment experiencing high traffic volume. DOY, day of year.

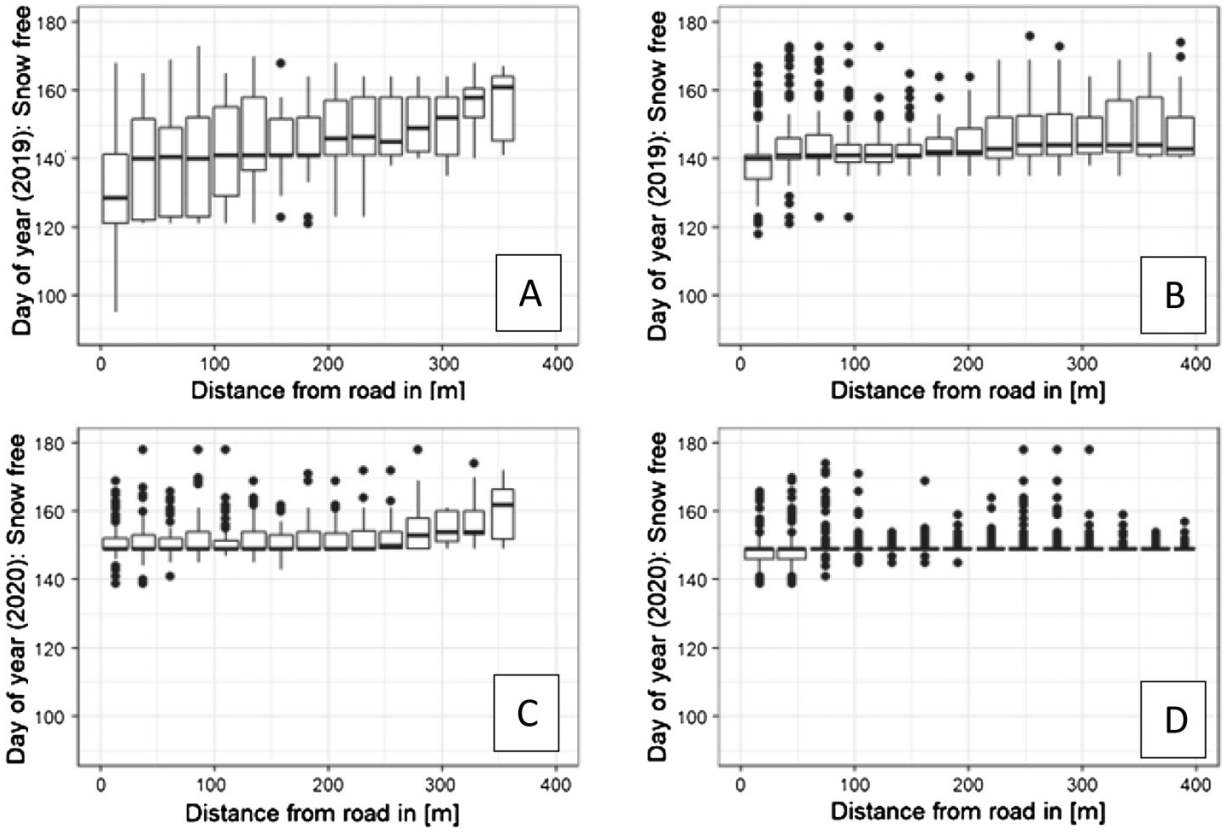

Analysing snow-free dates revealed general patterns of similar median snow-free dates, independent of distance to the nearest roads and pipelines (see Figs. 5 and 6). However, pixels within 5 km of the nearest road frequently showed outliers of earlier snow-free dates and in general a higher variability of snow-free timing compared to locations with greater distance to the nearest road segment. This suggests that while the proximity to roads does not necessarily lead to an earlier snow-free date, there is variability in snow-free timing introduced to the overall snowmelt progression by the presence of infrastructure, in particular roads (e.g., greater snow in deep drift areas and less snow in heavily dusted areas). Distinguishing between highly trafficked snow-free roads and smaller roads which typically experience lower usage revealed similar patterns to the analysis including all road types (compare Figs. 5, 6, and 7).

The classification of infrastructure according to winter snow cover (February–March) Sentinel-2 NDSI values revealed distinct differences between the main roads (e.g., Dalton Highway and Spine Road) and roads that experience less traffic, as well as pipelines and other types of infrastructure (see Figs. 2 and 8). While features like the Spine Road showed up in the classification as snow-free prior to general snowmelt onset, most other features were snow covered. Several main roads, including the Spine Road, are either transformed into ice roads during the winter by maintenance crews or naturally develop an ice layer due to compacted snow through high traffic. These roads are likely to melt out quickly due to sublimation and gravel may quickly come to the surface in spring before general snowmelt onset on the rest of the landscape. Features like the airport runway, which was classified as snow free, are purposefully kept snow free over the course of the winter. Other types of infrastructure, like gravel pits, pump stations, and gravel pads, were partially snow free. These features are often actively used during winter and are kept partially snow free or become snow free due to frequent machine activity. On pads, snow is removed from the portion of the pad that vehicles need to access. Throughout the winter, crews clear snow off the ice layer on pads and put it on the tundra to minimize mud on pads during the break up season. Snow will pile up around infrastructure in areas that are not drivable. According to information given during the interview with Hilcorp's field operations' supervisor for oilfield roads and pads, these results agree with their general observations (P. McCollor, personal communication, 2021). In their first-hand experience, areas with the most traffic melt earliest and roads that are elevated above the surrounding terrain are naturally cleared of snow by wind more quickly than those close to tundra level. Main roads (primary and flowline roads) are constructed at a minimum of 4 feet (approximately 1.2 m) above tundra, which helps to insulate the permafrost (by maintaining a frost bulb high up into

Fig. 8. Infrastructure in the Prudhoe Bay area and the respective snow cover levels for periods pre-snowmelt (February–March, 2019 and 2020) based on Sentinel-2 NDSI (sources for grey basemap: Esri, DeLorme, HERE, MapmyIndia) (WGS84/Alaska Polar Stereographic). NDSI, Normalized Difference Snow Index.

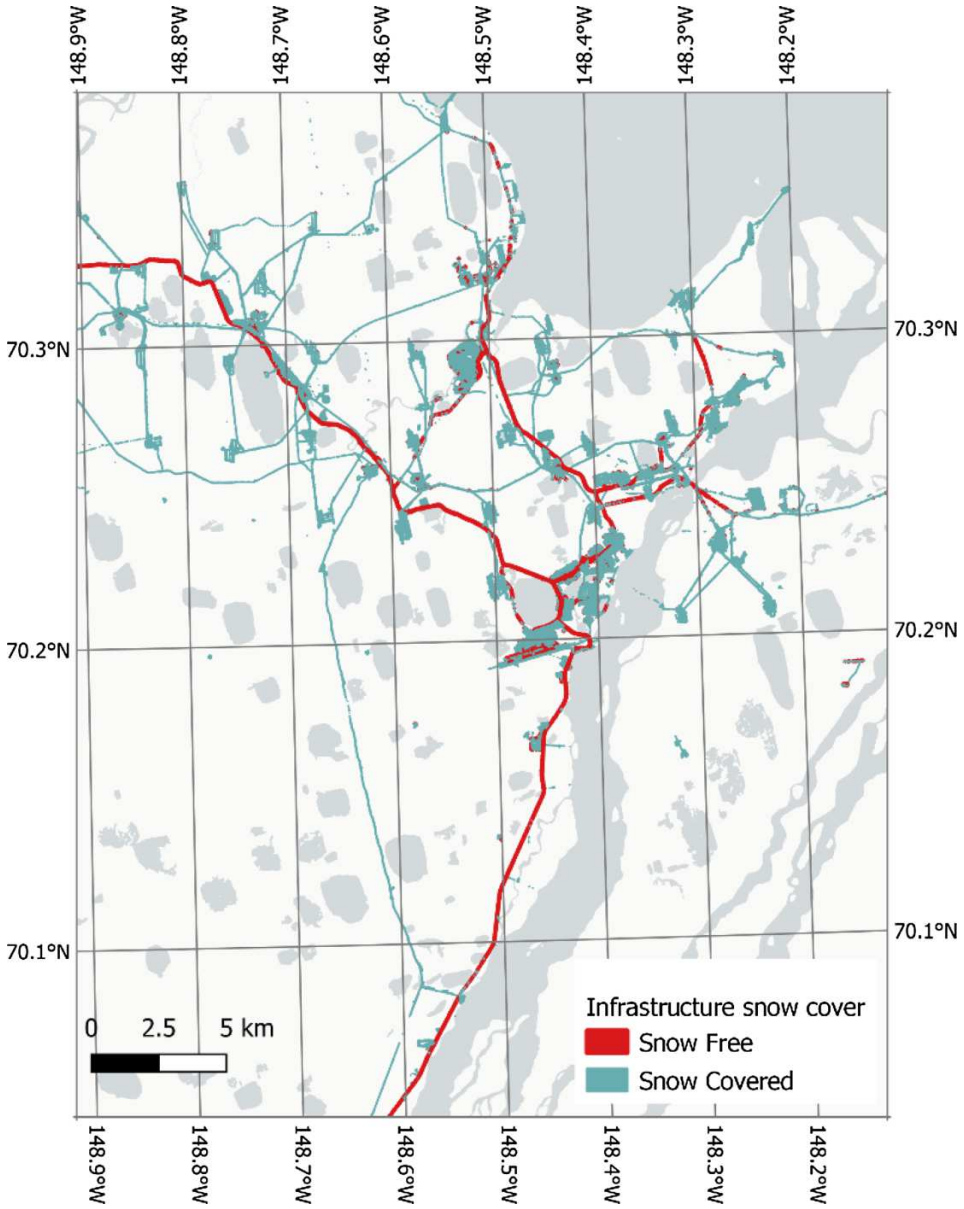

the road) and keeps the road surface harder longer. Smaller roads are built closer to the tundra level and do not get a lot of maintenance; both factors would suggest later snow off dates.

Localized melting occurs in areas where gravel protrudes through the ice. Road maintenance crews see steam coming off roads in winter, especially where gravel is emergent. On pads, snow is removed only from the portion of the pad that vehicles need to access. Around April 15, maintenance crews start stripping ice and snow off roads and drill site pads. Primary and flowline roads are intentionally iced in October for dust abatement, and maintenance crews water the roads throughout the winter to keep the ice built up. Ice paving is not done on oilfield access roads or on paved sections of the Dalton Highway, which include the last 52 miles coming into Deadhorse, where paving was completed in 2020–2021. Alaska DOT&PF uses ice paving on all non-asphalt sections of the Dalton Highway south to Milepost 209. Few sections of road within the oilfield are paved. Around 15 April, maintenance crews start stripping ice and snow off roads and drill site pads (W.J. Russel, personal communication, 2021).

Wind during the winter season is known to be a major influence on snow distribution and redistribution (Pomeroy et al. 2006). The combination of a predominant wind direction and infrastructure acting as artificial barriers on the relatively flat landscape results in snow build up along roads and increased snow depth (Fortier et al. 2011). This influences

Fig. 9. Daily mean ground surface temperature, grouped by months, January–July 2016, for Transects 1–4, Prudhoe Bay, Alaska. Temperatures were warmer closer to the road (left side of charts) at Transects 1, 2, and 4 for the winter months (1–3, January through March) compared to snow-free months.

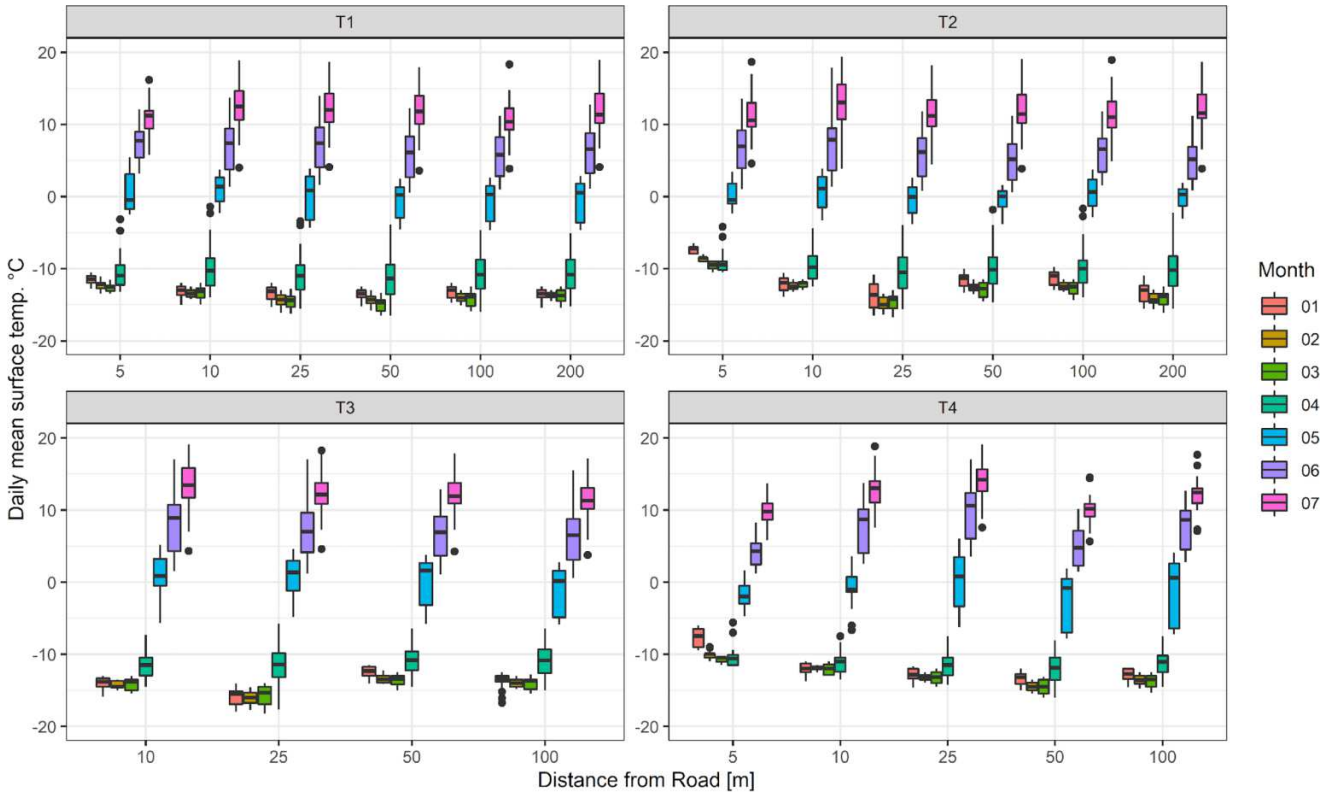

the snow-free timing, as the areas with increased snow depth tend to take longer to become fully snow free. Simultaneously, dust from snow-free infrastructure or natural sources (e.g., dust emanating from the Sagavanirktok River banks) is distributed by the wind as well, and deposited along raised infrastructure segments such as elevated roadbeds. Dust on the snow changes the albedo and can lead to increased snowmelt for a specific location. Considering both the increased snow depths caused by snow redistribution through wind and the effect of dust causing earlier snowmelt, wind leads to two distinct influences on snow that have the opposite effect on snowmelt timing. The higher variability in snowmelt timing near roads shown in our results (Fig. 5) agrees with these general observations and past research (e.g., Fortier et al. 2011). Water area derived from NDWI showed strong correlation with the distance to infrastructure for roads, pipelines, and other infrastructure areas within the study area (Fig. 15). The strong connection between water area and distance to infrastructure suggests a connection of delayed snowmelt, road-related damming affecting the cross-drainage of water, and increased thermokarst ponding and snow depth close to the road (Fig. 10) increasing the amount of water from snowmelt. In addition to the increased snow depth, infrastructure also provides barriers to surface drainage of melt water, creating conditions for early season flooding (Walker et al. 2022).

Influences from infrastructure on the natural landscape are varied and touch other natural processes in addition to snowmelt, including ice-wedge degradation, both natural and triggered by construction, a process which is prevalent in our study region (Raynolds et al. 2014; Kanevskiy et al. 2022). Deepening of ice-wedge troughs caused by ice-wedge degradation are areas of greater snow accumulation, and can be seen in the snow depth measurements along the individual transects (Fig. 10). Variables such as surface water area can be influenced by infrastructure through a change in surface hydrology, particularly in low-lying drained lake basin landforms, where water-pooling is exacerbated by the linear infrastructure. Vegetation parameters such as greenness and general productivity are influenced by water and dust distribution during the growing season (Ackerman and Finlay 2019). However, those variables are highly dependent on each other with differences in snowmelt patterns influencing post-snowmelt flooding and ponding along infrastructure. NDVI values show no clear connection to distance from roads or pipelines (Fig. 12) but show differences in seasonal NDVI progression between upwind and downwind areas adjacent to roads (Fig. 13). The interdependency of these factors makes it difficult to separate direct influences from infrastructure (such as acting as a snow fence or a source of dust) and the influence these variables have on each other (such as increased snow depth leading to more water near

Fig. 10. Snow depth in March 2016 vs. distance from road, for Transects 1–4, Prudhoe Bay (combining all transects in Panel A, separating transects in lower panels (T1, T2, T3, and T4).

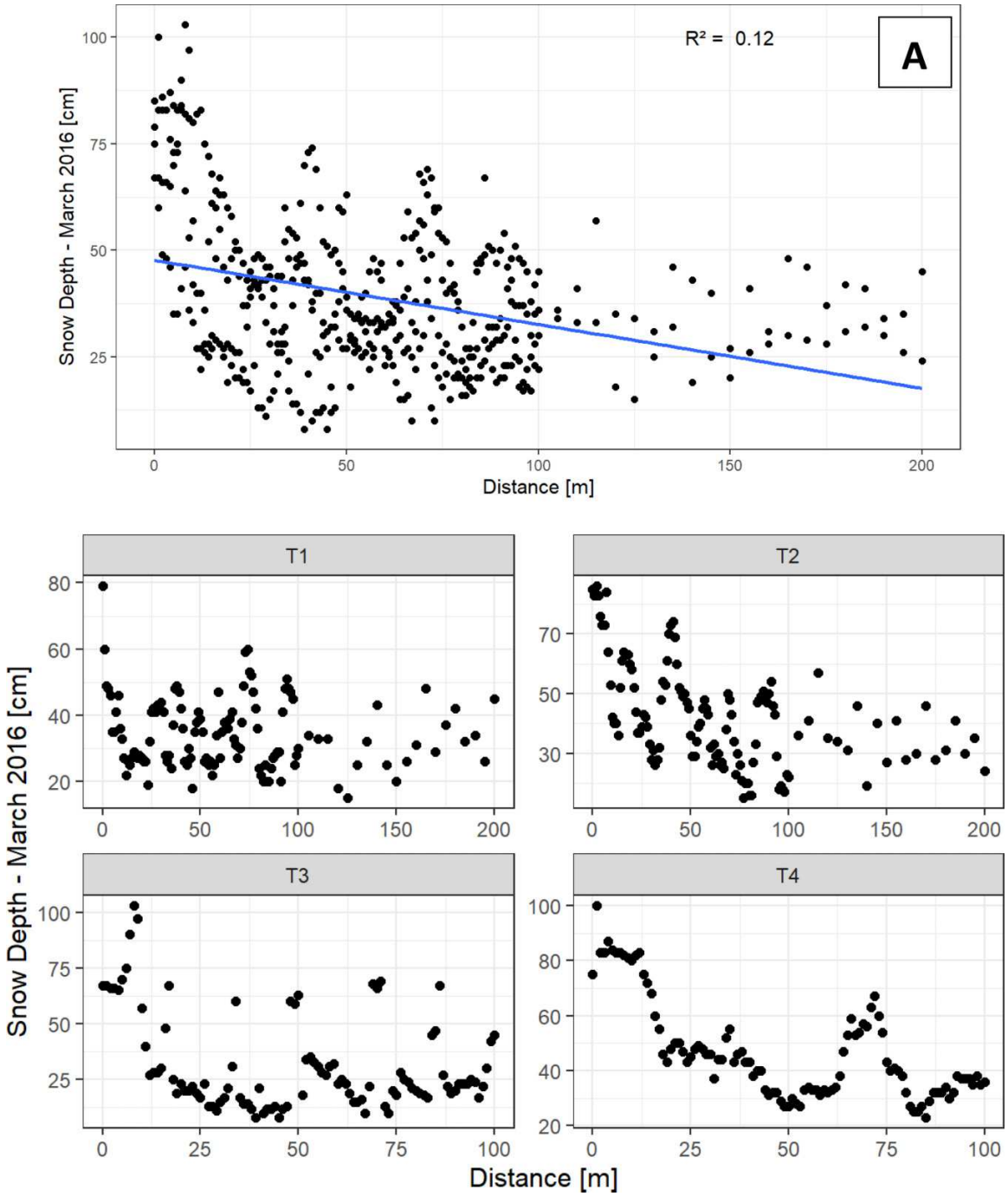

infrastructure or later snowmelt leading to a delay in NDVI increase).

5 Conclusion

The availability of relatively high-resolution satellite imagery (Sentinel-2) and the access to relatively high-resolution infrastructure data proved to be essential for the quantification of spatial and temporal patterns of snowmelt timing in relation to infrastructure elements. This study shows the suitability of multispectral Sentinel-2 data to study spatial patterns of snowmelt timing in Arctic industrial areas. This study highlights the impact of infrastructure on a large area extending past the direct human footprint as well as the interconnectedness between vegetation, hydrology, and near-surface ground temperatures. The influence of infrastructure on different environmental factors was shown to be highly variable both spatially and temporally and interdependent on each other. The availability of relatively

Fig. 11. Wind speeds and wind directions for Deadhorse station (retrieved from National Oceanic and Atmospheric Administration (NOOA) download center as daily mean values) for months (left) and years (right).

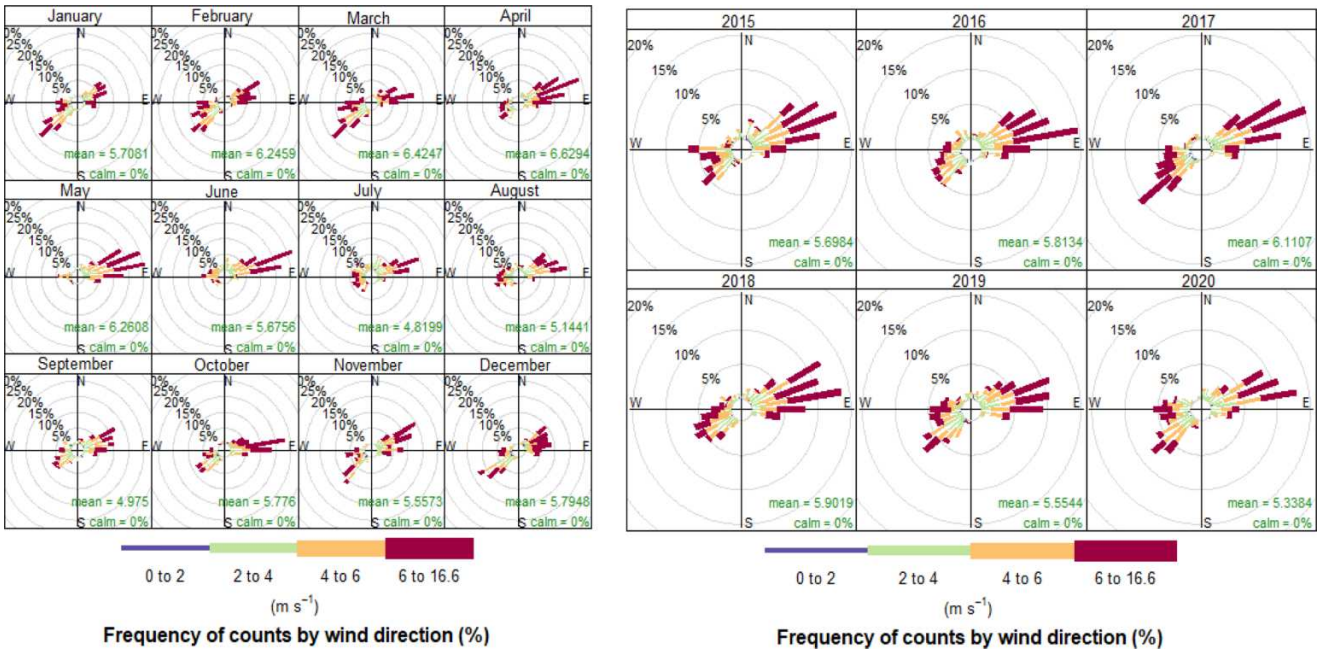

Fig. 12. Median NDVI values for June 2016–2020 in relation to distance to roads (A) and pipelines (B). NDVI, Normalized Difference Vegetation Index.

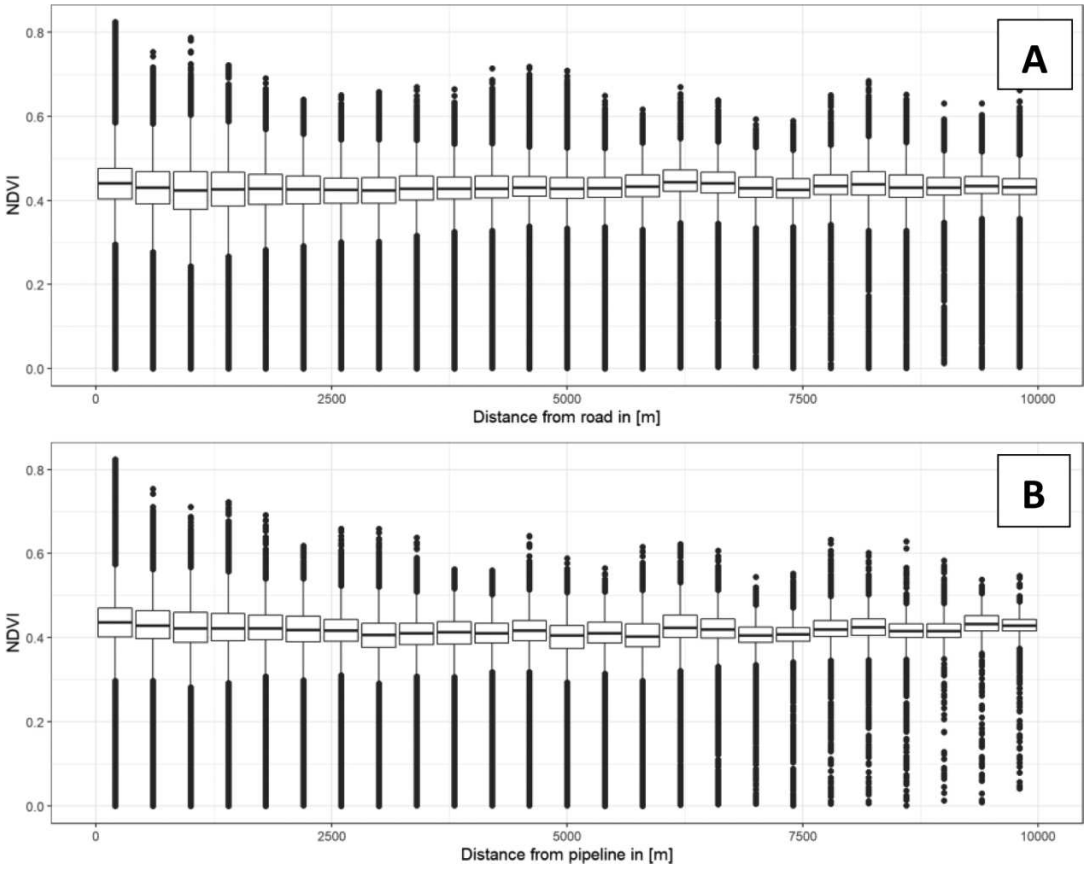

Fig. 13. NDVI for days of year for 2019–2020 for upwind and downwind areas along roads in the Prudhoe Bay study area. NDVI, Normalized Difference Vegetation Index.

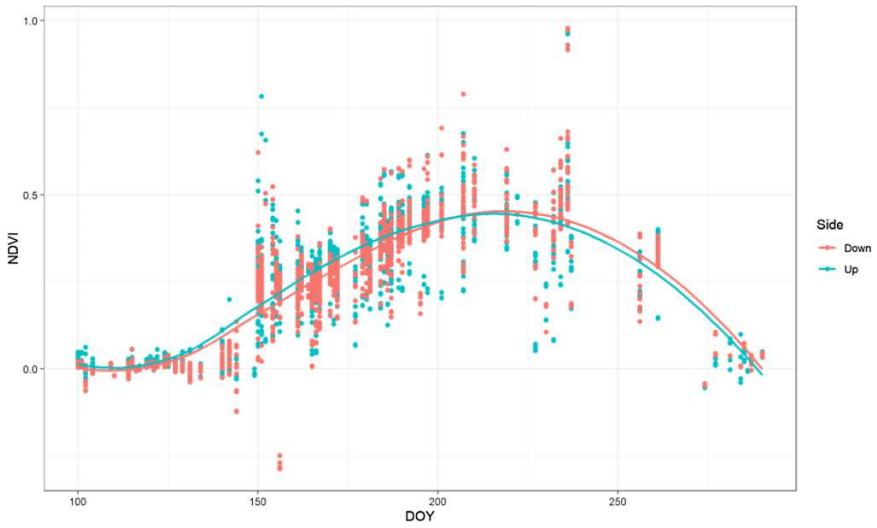

Fig. 14. Seasonal maximum NDVI values in the study area in relation to the DOY of first snow-free day for 2019 and 2020 per Sentinel-2 pixel. Boxplots per day of year. DOY, day of year; NDVI, Normalized Difference Vegetation Index.

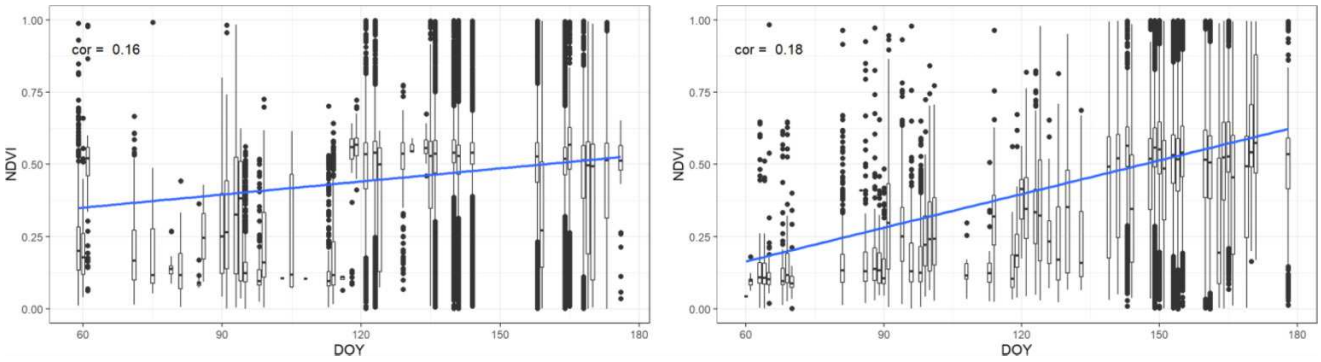

Fig. 15. Surface water area after snowmelt in square meters (June) in relation to distance from roads, pipelines, other infrastructure areas (excluding lakes and other permanent water areas). Area calculated for distance binned into 50 m bins.

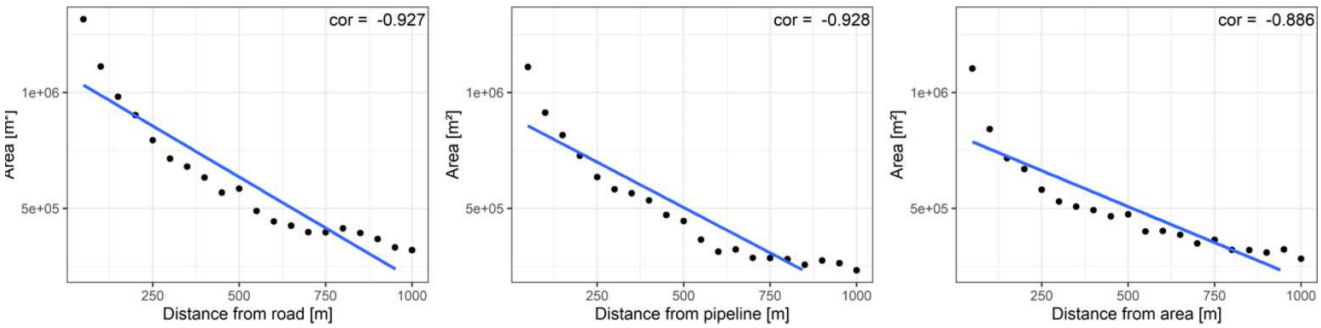

high-resolution satellite imagery as well as relatively high-resolution infrastructure data proved to be essential in visualizing and quantifying spatial patterns in snowmelt in relation to infrastructure elements. Snow-free dates vary strongly with their distance to infrastructure, especially roads with downwind and upwind areas experienced different snow and dust effects. Both vegetation and surface water indices (NDVI and NDWI, respectively) were shown to be correlated to distance to infrastructure. Our study shows that the presence of infrastructure introduces variability in snowmelt timing

Fig. 16. Photos showing snowmelt patterns for different positions in and around Prudhoe Bay. Photo A (by Martha Raynolds, June 2014, published in Walker et al. 2014) illustrates that many of the pipelines in Fig. 3 are composed of multiple parallel pipes that, in combination with an adjacent access road, create large snow drifts and affect large areas of tundra. Photo B (by Benjamin M. Jones, June 2014) shows a section of the Trans-Alaska Pipeline System and late-melting snowdrifts. This delayed snowmelt along the pipeline is clearly shown in Fig. 4 (yellow lines near the middle of both images).

and related phenomena in Arctic areas such as increased near-surface ground temperatures. The resulting interacting effects are complex and difficult to separate. It is clear, however, that the presence of infrastructure directly and indirectly modifies patterns of landscape change in Arctic areas.

Acknowledgements

We would like to thank Pat McCollor (field operations supervisor) from ASRC Energy Services and William J. Russel from Alaska DOT&PF (Northern Region Maintenance and Operation) for their input and the fruitful discussions of early results of this study.

Article information

History dates

Received: 28 February 2022
Accepted: 10 July 2022
Accepted manuscript online: 11 August 2022
Version of record online: 5 December 2022

Notes

This paper is part of a Collection entitled "Terrestrial Geosystems, Ecosystems, and Human Systems in the Fast-Changing Arctic".

Copyright

Data availability

Data generated or analyzed during this study are available from the corresponding author upon reasonable request.

Author information

Author ORCIDs

Helena Bergstedt https://orcid.org/0000-0003-4044-4792
Donald Walker https://orcid.org/0000-0001-9581-7811
Mikhail Kanevskiy https://orcid.org/0000-0003-0565-0187

Author contributions

H.B.:Conceptualization, Data curation, Formal analysis, Investigation, Methodology, Validation, Visualization, Writing – original draft, Writing – review & editing. B.M.J.: Conceptualization, Project administration, Supervision, Writing – original draft, Writing – review & editing. D.A.W.: Conceptualization, Funding acquisition, Project administration, Resources, Supervision, Writing – original draft, Writing – review & editing. J.L.P.: Methodology, Project administration, Writing – original draft. A.B.: Data curation, Funding acquisition, Supervision, Writing – original draft, Writing – review & editing. G.P.: Data curation, Writing – original draft. M.Z.K.: Conceptualization, Supervision, Writing – original draft. M.K.R.: Methodology, Writing – original draft. M.B.: Data curation, Writing – original draft.

Competing interests

The authors declare there are no competing interests.

Funding

Support for this study came from the US National Science Foundation (grant numbers: 1928237 and 1263854). In addition, work was funded through the European Union's Horizon 2020 Research and Innovation Program (grant agreement number: 773421).

References

Aalstad, K., Westermann, S., and Bertino, L. 2020. Evaluating satellite retrieved fractional snow-covered area at a high-Arctic site using terrestrial photography. Remote Sens. Environ. **239**: 111618. doi:10.1016/j.rse.2019.111618.

Ackerman, D.E., and Finlay, J.C. 2019. Road dust biases NDVI and alters edaphic properties in Alaskan Arctic tundra. Sci. Rep. **9**(1): 1–8. doi:10.1038/s41598-018-36804-3. PMID: 30626917.

AMAP Assessment 2007. *Oil and Gas Activities in the Arctic—Effects and Potential Effects*, Arctic Monitoring and Assessment Programme (AMAP), Oslo, Norway. Available from: https://www.amap.no/documents/doc/assessment-2007-oil-and-gas-activities-in-the-arctic-effects-and-potential-effects.-volume-2/100.

Andrews, J.T., Davis, P.T., and Wright, C. 1976. Little ice age permanent snowcover in the eastern canadian arctic: extent mapped from landsat-1 satellite imagery. Geogr. Ann. Ser. A **58**(1-2): 71–81. doi:10.1080/04353676.1976.11879925.

Bartsch, A., Pointner, G., and Nitze, I. 2021b. Sentinel-1/2 derived arctic coastal human impact dataset (SACHI) Zenodo. Available from: https://zenodo.org/record/4925911.

Bartsch, A., Pointner, G., Ingeman-Nielsen, T., and Lu, W. 2020. Towards circumpolar mapping of Arctic settlements and infrastructure based on sentinel-1 and Sentinel-2. Remote Sens. **12**(15): 2368. doi:10.3390/rs12152368.

Bartsch, A., Pointner, G., Nitze, I., Efimova, A., Jakober, D. Ley, S., et al. 2021a. Expanding infrastructure and growing anthropogenic impacts along Arctic coasts. Environ. Res. Lett. **16**(11): 115013. doi:10.1088/1748-9326/ac3176.

Benson, C., Holmgren, B., Timmer, R., Weller, G., and Parrish, S. 1975. Observations on the seasonal snow cover and radiation climate at prudhoe bay, Alaska during 1972. Ecological investigations of the tundra biome in the prudhoe bay region, Alaska. Biol. Papers Univ. Alaska. Special report. (2): 12–50.

Berman, E.E., Bolton, D.K., Coops, N.C., Mityok, Z.K., Stenhouse, G.B., and Moore, R.D. 2018. Daily estimates of landsat fractional snow cover driven by MODIS and dynamic time-warping. Remote Sens. Environ. **216**: 635–646. doi:10.1016/j.rse.2018.07.029.

Chaponniere, A., Maisongrande, P., Duchemin, B., Hanich, L., Boulet, G., Escadafal, R., and Elouaddat, S. 2005. A combined high and low spatial resolution approach for mapping snow covered areas in the Atlas Mmountains. Int. J. Remote Sens. **26**(13): 2755–2777. doi:10.1080/01431160500117758.

Chen, L., Fortier, D., McKenzie, J.M., and Sliger, M. 2020. Impact of heat advection on the thermal regime of roads built on permafrost. Hydrol. Process. **34**(7): 1647–1664. doi:10.1002/hyp.13688.

Dietz, A.J., Kuenzer, C., Gessner, U., and Dech, S. 2012. Remote sensing of snow–a review of available methods. Int. J. Remote Sens. **33**(13): 4094–4134. doi:10.1080/01431161.2011.640964.

Dozier, J. 1984. Snow reflectance from landsat-4 thematic mapper. IEEE Trans. Geosci. Remote Sens. **GE-22**(3): 323–328. doi:10.1109/TGRS.1984.350628.

Dozier, J. 1989. Spectral signature of alpine snow cover from the landsat thematic mapper. Remote Sens. Environ. **28**: 9–22. doi:10.1016/0034-4257(89)90101-6.

Drusch, M., Del Bello, U., Carlier, S., Colin, O., Fernandez, V. Gascon, F., et al. 2012. Sentinel-2: ESA's optical high-resolution mission for GMES operational services. Remote Sens. Environ. **120**: 25–36. doi:10.1016/j.rse.2011.11.026.

Du, Y., Zhang, Y., Ling, F., Wang, Q., Li, W., and Li, X. 2016. Water bodies' mapping from sentinel-2 imagery with modified normalized difference water index at 10-m spatial resolution produced by sharpening the SWIR band. Remote Sensing, **8**(4): 354. doi:10.3390/rs8040354.

Esch, T., Bachofer, F., Heldens, W., Hirner, A., Marconcini, M. Palacios-Lopez, D., et al. 2018. Where we live—a summary of the achievements and planned evolution of the global urban footprint. Remote Sens. **10**(6): 895. doi:10.3390/rs10060895.

Everett, K.R. 1980. Distribution and properties of road dust along the northern portion of the haul road. Environmental engineering and ecological baseline investigations along the Yukon River-Prudhoe Bay Haul Road. CRREL Report, pp. 80–19. Hanover, New Hampshire, USA.

Everett, K.R., and Parkinson, R.J. 1977. Soil and landform associations, prudhoe bay area, Alaska. Arct. Alp. Res. **9**(1): 1–19. doi:10.2307/1550406.

Fortier, R., LeBlanc, A.M., and Yu, W. 2011. Impacts of permafrost degradation on a road embankment at umiujaq in Nunavik (Quebec), Canada. Can. Geotech. J. **48**(5): 720–740. doi:10.1139/t10-101.

Frei, A., Tedesco, M., Lee, S., Foster, J., Hall, D.K., Kelly, R., and Robinson, D.A. 2012. A review of global satellite-derived snow products. Adv. Space Res. **50**(8): 1007–1029. doi:10.1016/j.asr.2011.12.021.

Gascoin, S., Barrou Dumont, Z., Deschamps-Berger, C., Marti, F., Salgues, G. López-Moreno, J.I., et al. 2020. Estimating fractional snow cover in open terrain from sentinel-2 using the normalized difference snow index. Remote Sensing, **12**(18): 2904. doi:10.3390/rs12182904.

Gascon, F., Bouzinac, C., Thépaut, O., Jung, M., Francesconi, B. Louis, J., et al. 2017. Copernicus Sentinel-2A calibration and products validation status. Remote Sens. **9**(6): 584. doi:10.3390/rs9060584.

Hall, D.K., and Riggs, G.A. 2007. Accuracy assessment of the MODIS snow products. Hydrol. Process. **21**(12): 1534–1547. doi:10.1002/hyp.6715.

Hall, D.K., Riggs, G.A., Salomonson, V.V., DiGirolamo, N.E., and Bayr, K.J. 2002. MODIS snow-cover products. Remote Sens. Environ. **83**(1-2): 181–194. doi:10.1016/S0034-4257(02)00095-0.

Hu, Z., Dietz, A., and Kuenzer, C. 2019. The potential of retrieving snow line dynamics from landsat during the end of the ablation seasons between 1982 and 2017 in european mountains. Int. J. Appl. Earth Obs. Geoinf. **78**: 138–148. doi:10.1016/j.jag.2019.01.010.

Kanevskiy, M., Shur, Y., Walker, D.A., Jorgenson, M.T., Jones, B.M. Buchhorn, M., et al. 2022. The shifting mosaic of ice-wedge degradation and stabilization in response to infrastructure and climate change, prudhoe bay oilfield, Alaska. Arct. Sci. **8**: 498–530. doi:10.1139/AS-2021-0024.

Kępski, D., Luks, B., Migała, K., Wawrzyniak, T., Westermann, S., and Wojtuń, B. 2017. Terrestrial remote sensing of snowmelt in a diverse high-Arctic tundra environment using time-lapse imagery. Remote Sens. **9**(7): 733. doi:10.3390/rs9070733.

Kumpula, T., Forbes, B.C., Stammler, F., and Meschtyb, N. 2012. Dynamics of a coupled system: multi-resolution remote sensing in assessing social-ecological responses during 25 years of gas field development in arctic russia. Remote Sensing, **4**(4): 1046–1068. doi:10.3390/rs4041046.

Macander, M.J., Swingley, C.S., Joly, K., and Raynolds, M.K. 2015. Landsat-based snow persistence map for northwest Alaska. Remote Sens. Environ. **163**: 23–31. doi:10.1016/j.rse.2015.02.028.

Nitze, I., and Grosse, G. 2016. Detection of landscape dynamics in the Arctic lena delta with temporally dense landsat time-series stacks. Remote Sens. Environ. **181**: 27–41. doi:10.1016/j.rse.2016.03.038.

NRC (National Research Council). 2003. *Cumulative Environmental Effects of Oil and Gas Activities on Alaska's North Slope*, National Academies Press. Washington, DC, USA. doi:10.17226/10639.

Pomeroy, J.W., Bewley, D.S., Essery, R.L., Hedstrom, N.R., Link, T. Granger, R.J., et al. 2006. Shrub tundra snowmelt. Hydrol. Process. **20**(4): 923–941. doi:10.1002/hyp.6124.

Raynolds, M.K., Jorgenson, J.C., Jorgenson, M.T., Kanevskiy, M., Liljedahl, A.K. Nolan, M., et al. 2020. Landscape impacts of 3D-seismic surveys in the arctic national wildlife refuge, Alaska. Ecol. Appl. **30**(7): e02143. doi:10.1002/eap.2143. PMID: 32335990.

Raynolds, M.K., Walker, D.A., Ambrosius, K.J., Brown, J., Everett, K.R. Kanevskiy, M., et al. 2014. Cumulative geoecological effects of 62 years of infrastructure and climate change in ice-rich permafrost landscapes, Prudhoe Bay Oilfield, Alaska. Global Change Biol. **20**(4): 1211–1224. doi:10.1111/gcb.12500. PMID: 24339207.

Salomonson, V.V., and Appel, I. 2004. Estimating fractional snow cover from MODIS using the normalized difference snow index. Remote Sens. Environ. **89**(3): 351–360. doi:10.1016/j.rse.2003.10.016.

Takala, M., Luojus, K., Pulliainen, J., Derksen, C., Lemmetyinen, J. Kärnä, J.P., et al. 2011. Estimating northern hemisphere snow water equivalent for climate research through assimilation of space-borne radiometer data and ground-based measurements. Remote Sens. Environ. **115**(12): 3517–3529. doi:10.1016/j.rse.2011.08.014.

Truett, J.C., Mark, E.M., and Kenneth, K. 1997. Effects of Arctic Alaska Oil Development on Brant and Snow Geese." Arctic 50, no. 2. 138–46. Available from http://www.jstor.org/stable/40512084.